ELSEVIER

Biophysical Chemistry 95 (2002) 135–144

Biophysical Chemistry

www.elsevier.com/locate/bpc

The application of fluorescence correlation spectroscopy in detecting DNA condensation

Teresa Kral[a,b,*], Marek Langner[c,d], Martin Beneš[b], Dagmara Baczyńska[e], Maciej Ugorski[e], Martin Hof[b]

[a]*Agricultural University, Department of Physics and Biophysics, Norwida 25, 50-375 Wrocław, Poland*
[b]*J. Heyrovský Institute of Physical Chemistry, Academy of Sciences of the Czech Republic and Center for Complex Molecular Systems and Biomolecules, Dolejškova 3, 18223 Prague, Czech Republic*
[c]*Wrocław University of Technology, Institute of Physics, Wyb. Wyspiańskiego 27, 50-370, Wrocław, Poland*
[d]*Center of Biotechnology of Lipids Aggregates, Przybyszewskiego 63/67 51-148 Wrocław, Poland*
[e]*Department of Immunochemistry, Ludwik Hirszfeld Institute of Immunology and Experimental Therapy, Polish Academy of Science, R. Weigla 12, 53-114 Wrocław, Poland*

Received 25 September 2001; received in revised form 5 December 2001; accepted 7 December 2001

Abstract

We report the application of fluorescence correlation spectroscopy (FCS) in characterizing conformational changes (condensation) of chemically well-defined DNA plasmids. The plasmids: pHβAPr-1-neo (10 kbp, contour length 3.4 μm) and pBluescript SKt (2.96 kbp, contour length 1.02 μm) were imaged by a confocal fluorescence microscope using two fluorescent probes: ethidium bromide (EtBr) and propidium iodide (PrIo). It became clear that the DNA molecule exhibits discrete conformational change between the coil and globule states with the addition of a small amount (the order of magnitude being 10^{-5} M) of cationic surfactant, spermine and hexadecyltrimethyl ammonium bromide (HTAB). When the concentrations of both condensing agents are smaller than 6.0×10^{-6} M and 2.0×10^{-6} M for the 10 and 2.96 kbp, both plasmids are in the extended coil state with diffusion constants $D_{10\ kbp}=9.6\times10^{-13}$ m^2 s^{-1} and $D_{2.96\ kbp}=2.5\times10^{-12}$ m^2 s^{-1}, respectively. When the condensing agent in a concentration higher than 1.10×10^{-5} M is added to pHβAPr-1-neo (10 kbp), plasmids are in the condensed globular state and their diffusion constants are $D_{10\ kbp}=8.0\times10^{-12}$ m^2 s^{-1} (spermine) and $D_{10\ kbp}=5.5\times10^{-12}$ m^2 s^{-1} (HTAB). The globular state of the pBluescript SKt (2.96 kbp) plasmids is characterized by diffusion constants equal to $D_{2.96\ kbp}=9.2\times10^{-12}$ m^2 s^{-1} (spermine) and $D_{2.96\ kbp}=8.2\times10^{-12}$ m^2 s^{-1} (HTAB).

Keywords: Plasmid condensation; Ethidium bromide; Propidium iodide; FCS; Spermine; Hexadecyltrimethyl ammonium bromide

*Corresponding author. Tel.: +48-71-320-5275; fax: +48-71-320-5172.
E-mail address: tek@ozi.ar.wroc.pl (T. Kral).

0301-4622/02/$ - see front matter
PII: S0301-4622(01)00253-8

1. Introduction

Gene therapy is an emerging therapeutic approach based on the delivery of genetic material to the cells whose function is to be modified. The DNA molecule is a large and highly charged polyion, hence alone it is unable to penetrate the plasma membrane barrier and reach the nucleus, where the information that it carries needs to be delivered. Furthermore, when introduced to circulation or tissue, the DNA molecule becomes subject to instantaneous hydrolysis by nucleases. For such reasons, an appropriate delivery vehicle that would overcome these problems is needed. Non-viral gene carriers have become one of the main vehicles under consideration for this task [1–3]. The construction of an aggregate containing DNA requires detailed knowledge of the processes leading to its formation and the precise characterization of the resulting structure. This knowledge is still fragmentary, thus the design and formation of such aggregates is based on semi-empirical and poorly reproducible procedures [4–6].

The process of lipid-DNA aggregate formation can be intuitively divided into two stages: the condensation of the DNA molecule and its subsequent or simultaneous association with amphiphilic compounds [7]. The resulting aggregate should have well-defined and reproducible topology in order to be useful for pharmacological applications. DNA condensation has been extensively studied both experimentally and theoretically [5,8–12]. Steady state fluorescence is routinely utilized for the detection of DNA and RNA. A myriad of fluorescent probes are used for this purpose, but two of them particularly frequently: propidium iodide; and ethidium bromide [13]. It has been shown that these dyes increase their fluorescence, upon association with the DNA molecule, and this can be utilized for detection and imaging purposes. When a multivalent cationic compound is added to an aqueous suspension of labeled DNA, the DNA collapses and releases the fluorescent dye. This effect is frequently used to monitor the condensation process. Steady state fluorescence experiments provide information that is average for the whole DNA population. Such measurements are frequently not informative enough, particularly when DNA is in a number of distinct conformational states and each state has different affinity towards the condensing agents and/or fluorescent label. In order to overcome this problem, a single molecule detection technique is needed. If the DNA is large enough, microscopic analysis can be used [10,14,15]. In this paper, we present data concerning DNA condensation measured with fluorescence correlation spectroscopy (FCS) for the first time. The technique is well suited for measuring molecule or aggregate size distribution and the number of fluorescent species present in the sample. For this reason FCS can be used to follow both changing hydrodynamic size and the fraction of DNA molecules that are associated with the fluorescent label.

2. Experimental

2.1. Plasmids and chemicals

Ethidium bromide (EtBr) and propidium iodide (PrIo) were purchased from Molecular Probes (Eugene, Oregon, USA); spermine and hexadecyltrimethyl ammonium bromide (HTAB) were obtained from Sigma.

Plasmids, pHβAPr-1-neo (10 kbp, contour length 3.4 μm) and pBluesript SKt (2.96 kbp, contour length 1.02 μm) were prepared as described [16] with some modification of purification step. Briefly, DNA was precipitated with isopropanol and the sample centrifuged at $12\,000 \times g$ for 5 min at room temperature. The pellet was dissolved in a solution of RNase A (10 μg/ml) and incubated for 15 min and then a sample was extracted once with phenol–chloroform–isoamyl alcohol (25:24:1, v/v/v) and twice with chloroform–isoamyl alcohol (24:1, v/v). Combined upper phases were precipitated with 5 M potassium acetate–isopropanol–water (1:22:2, v/v/v). After centrifugation, the DNA pellet was washed with 70% ethanol and re-dissolved in water.

2.2. Fluorescence correlation spectroscopy

All measurements were done on a ConfoCor 1 manufactured by Carl Zeiss Jena, Germany.

ConfoCor 1 is a PC-controlled fluorescence correlation-adapted AXIOVERT 135 TV microscope equipped with an x–y–z adjustable pinhole, avalanche Photodiode SPCM-200-PQ, ALV-hardware correlator and CCD camera. The Ar^+-laser beam (488 and 514 nm) was focused by a water-immersion microscope objective at an open focal light cell. The same objective, a dichroic mirror, proper bandpass filters and a pinhole in the image space block collected fluorescence light. The fluorescence intensity signal $I(t)$ fluctuating around a temporal average $[I(t)=\langle I(t)\rangle+\delta I(t)]$ was processed with a digital hardware correlator interface yielding the normalized autocorrelation function $G(t)$ $[G(t)=1+\langle \delta I(t)\delta I(t+\tau)\rangle/\langle I(t)\rangle^2]$. A general solution for the three-dimensional autocorrelation function $G(t)$ regarding translational diffusion in an ellipsoid confocal volume element yields the following formula for the situation that the fluorescence decay (τ_f) and translational diffusion τ_d are well separated in time ($\tau_f \ll \tau_d$):

$$G(t)=1+\frac{1}{N}\ \frac{1}{1+(t/\tau_D)}\times\left\{\frac{1}{1+(t/\tau_D)(\omega_1^2/\omega_2^2)}\right\}^{1/2} \quad (1)$$

where ω_1 is the radius of the volume element in xy plane, ω_2 is the half-length of the volume element in z direction and N is particle number. When knowing ω_1 and τ_D, the diffusion coefficient D can be determined ($\tau_D=\omega_1^2/4D$).

Since for both of the used dyes, intersystem crossing creates molecules in the triplet state that can be considered as non-fluorescent, an average fraction of dye molecules in the triplet state and an intersystem crossing relaxation time has to be included in the theoretical fitting function [Eq. (1)]. In the case when the resulting expression does not fit satisfactorily to experimental data, a term for a second diffusing species labelled with the same fluorophore can be included. Deviation and the exact formulation of these functions are described in detail in several review articles on FCS [17,18] and in a recent publication by our group [19].

FCS measurement samples were prepared as follows: an appropriate amount of DNA water solution was placed into the chamber, with the glass bottom facing the water-immersion microscope objective of the ConfoCor instrument. The plasmid stock solutions used in our experiment were an inhomogeneous mixture of the Nicked and supercoiled form of the both DNA (10 and 2.96 kbp, respectively, line b and d in Fig. 1). The fluorescent label was then added from a water stock solution (1×10^{-5} M), followed by titration with the condensing agent. Fluorescent probe concentrations were determined by spectroscopic measurements. All experiments were carried out at room temperature and in distillated and deionized water (pH 6.85)

3. Results and discussion

3.1. The detection of DNA labeled with fluorescent dye

Ethidium bromide and propidium iodide are one of the most widely used nucleic acid stains. They are known to bind to DNA by intercalation between base pairs with little sequence preference. Binding stochiometry was determined to be one dye molecule per four to five DNA base pairs [20]. The relatively poor fluorescence intensity of both dyes is known to be enhanced 20- to 30-fold upon binding to DNA [13,21,22].

FCS measurements on DNA molecules labeled with fluorescent dyes allow the straightforward determination of two parameters: (i) the particle number, N; (ii) diffusion time τ_d and thus also the molecule diffusion constant D. In addition, we made use of a directly measured parameter, count rate (CR). The dimensions of the volume element were determined to be $\omega_1=2.5\pm0.5\times10^{-7}$ m and $\omega_2=1.5\pm0.4\times10^{-6}$ m. Average fractions of both dye molecules in the triplet state were below 10%.

Experimental $G(t)$ functions were satisfactorily fitted to the theoretical expression of a diffusional system with a single fluorescent particle type and a certain amount of dye molecules in the triplet state ($<10\%$). An example of the autocorrelation functions with measured count rates and results of DNA (2.96 kbp) titration with fluorescent dyes are shown on Fig. 2 and Fig. 3, respectively. The measured diffusion constant and particle number

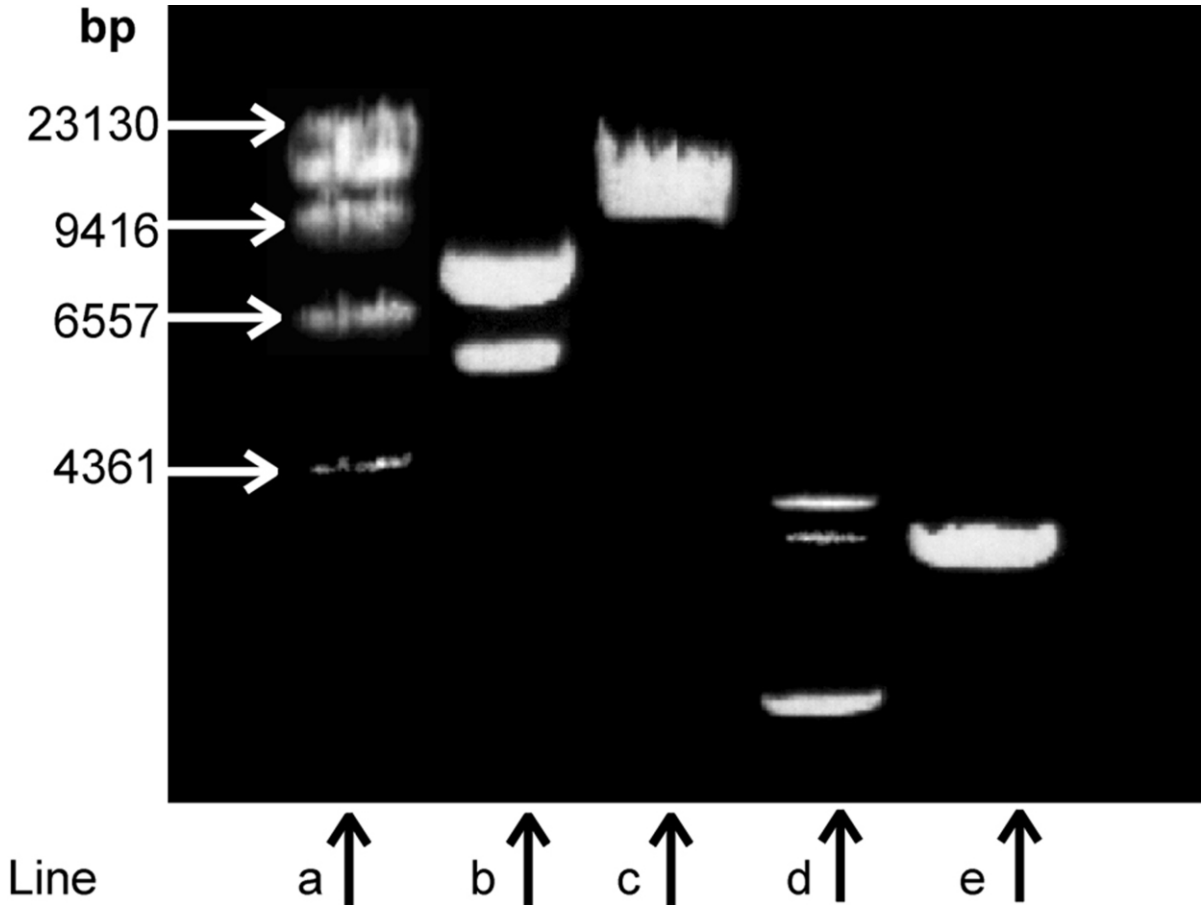

Fig. 1. Agarose gel electrophoresis of plasmids: Line a, Marker λDNA; Line b, pHβAPr-1-neo (10 kbp, contour length 3.4 μm, molecular mass (6.6×10^6); Line c, pH βApr-1-Neo + Hind III restriction enzyme; Line d, pBluesript SKt (2.96 kbp, contour length 1.02 μm), molecular mass (1.98×10^6); Line e, pBluesript SKt + Hind III restriction enzyme.

remain practically constant for the whole presented range of fluorescent dye concentration. Furthermore, there were no differences between EtBr and PrIo (Fig. 3a,b). However, count rate, reflecting the amount of fluorescence associated with single DNA molecules, changes with dye concentration. In addition, there is noticeable count rate difference between EtBr and PrIo, which must reflect higher fluorescence yield for bound ethidium bromide or a larger number of these dye molecules associated with DNA.

When the dye/DNA ratio was smaller than 100 (data not shown), the autocorrelation function $G(t)$ could no longer be satisfactorily fitted by the theoretical expression for a diffusional system with a single fluorescent particle type. When the theoretical description of two diffusing species labeled with the same fluorophore was applied, a second fast diffusion time comparable to those obtained for low-molecular weight components is obtained. The obtained diffusion coefficients calculated from the two diffusion times are $D_{2.96\ \mathrm{kbp}}=2.5\times10^{-12}$ $\mathrm{m^2\ s^{-1}}$ and $D_{\mathrm{dye}}=2.5\times10^{-10}\ \mathrm{m^2\ s^{-1}}$, respectively. In both cases standard deviation was approximately 25%. While the diffusion constant $D_{2.96\ \mathrm{kbp}}=2.5\times10^{-12}\ \mathrm{m^2\ s^{-1}}$ is identical to the diffusion constant resulting from monocomponent fits to the data obtained from dye/DNA values >100, the latter is similar to values obtained for low molecular weight compounds [19]. However, the fluo-

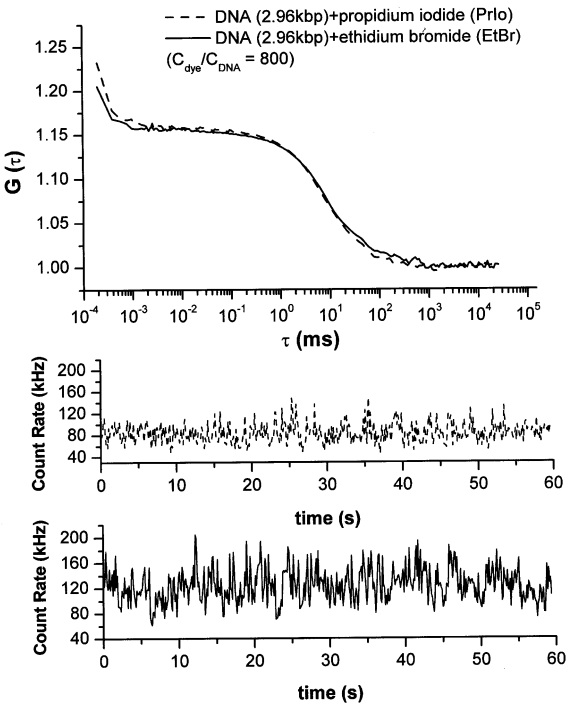

Fig. 2. Normalized fluorescence autocorrelation functions obtained for plasmid pBluesript SKt (2.96 kbp, contour length 1.02 μm) labeled with propidium iodide (dashed line) and ethidium bromide (continuous line). The C_{dye}/C_{DNA} ratio was equal 800. Corresponding fluorescence count rates are shown on the lower panels. Experimental $G(t)$ functions were satisfactorily fitted to the theoretical expression of a diffusional system with the one component model in the entire range. Triplet state was below 10%.

rescence intensity of nM concentrations of both dyes in bulk water is far too small to explain the occurrence of the fast diffusing component. This fact can be easily demonstrated by FCS measurements of both dyes in bulk water using dye concentrations comparable to those used in the DNA experiments (data not shown). A reviewer pointed out, that the origin of the two components could be two diffusional modes similar to those observed by dynamic light scattering measurements [20]. There are two arguments against such an interpretation: (1) While the diffusion constants determined by light scattering differ roughly by approximately a factor 10, we observe differences in the diffusion constants for fast and slow components of two orders of magnitude. (2) The appearance of the two components does not depend on the DNA concentration, but is strongly dependent on the dye concentration. In our opinion the deviation from the monophasic diffusional system at low dye concentrations is due to fluctuations in the number of dye molecules bound to a single DNA molecule, caused by the desorption of dye molecules. Since the quantum yield of an unbound dye molecule is much lower than that of a bound one, the fluctuations in the amount of bound dye molecules result in fluorescence fluctuations. This explanation is in line with our observation that these fluctuations become more pronounced with the decrease of the number of bound dye molecules. Apparently at dye/DNA ratios larger than 100 these fluctuations become much smaller than the fluctuations caused by DNA diffusion and, thus, are no longer detectable. In order to quantitatively evaluate this observation, a proper model needs to be constructed, similar to those presented in literature [17,23].

The obtained value of the diffusion constant for pBluescript SKt (2.96 kbp, contour length 1.02 μm) is equal $D_{2.96\ kbp}=2.5\times10^{-12}$ m^2 s^{-1} and is identical within the experimental error for both dyes (Fig. 3a). The experimentally derived value of the diffusion constant is in the similar range than the one calculated (3×10^{-12} m^2 s^{-1}), when hypothesizing a rod-like DNA molecule with 3.4 Å per base pair and a 23.8 Å diameter of the rod [24]. This calculation has been performed using the formula for the rigid rod translational diffusion coefficient given by Tirado and Garcia de la Torre [25]: $D=\frac{k_BT}{3\pi\eta_0L}\times(1n\ p+\nu)$, where $\nu=0.312+\frac{0.565}{p}-+\frac{0.1}{p^2}$, k_bT is the Bolzmann energy, $p=(L/d)$ is the ratio of the length to cross-section diameter, and η_0 is the viscosity of the solvent.

The diffusion coefficient for the 10 kbp plasmid (pHβApr-1-neo with a contour length of 3.4 μm) was determined to be equal 9.6×10^{-13} m^2 s^{-1} and again independent of the choice of the dye. If we apply the above calculation for this molecule we obtain an estimated diffusion coefficient of $D_{10\ kbp}=1\times10^{-12}$ m^2 s^{-1}.

We would like to point out that the above used 'rigid rod' model represents an oversimplification of the shape of the investigated DNA molecules.

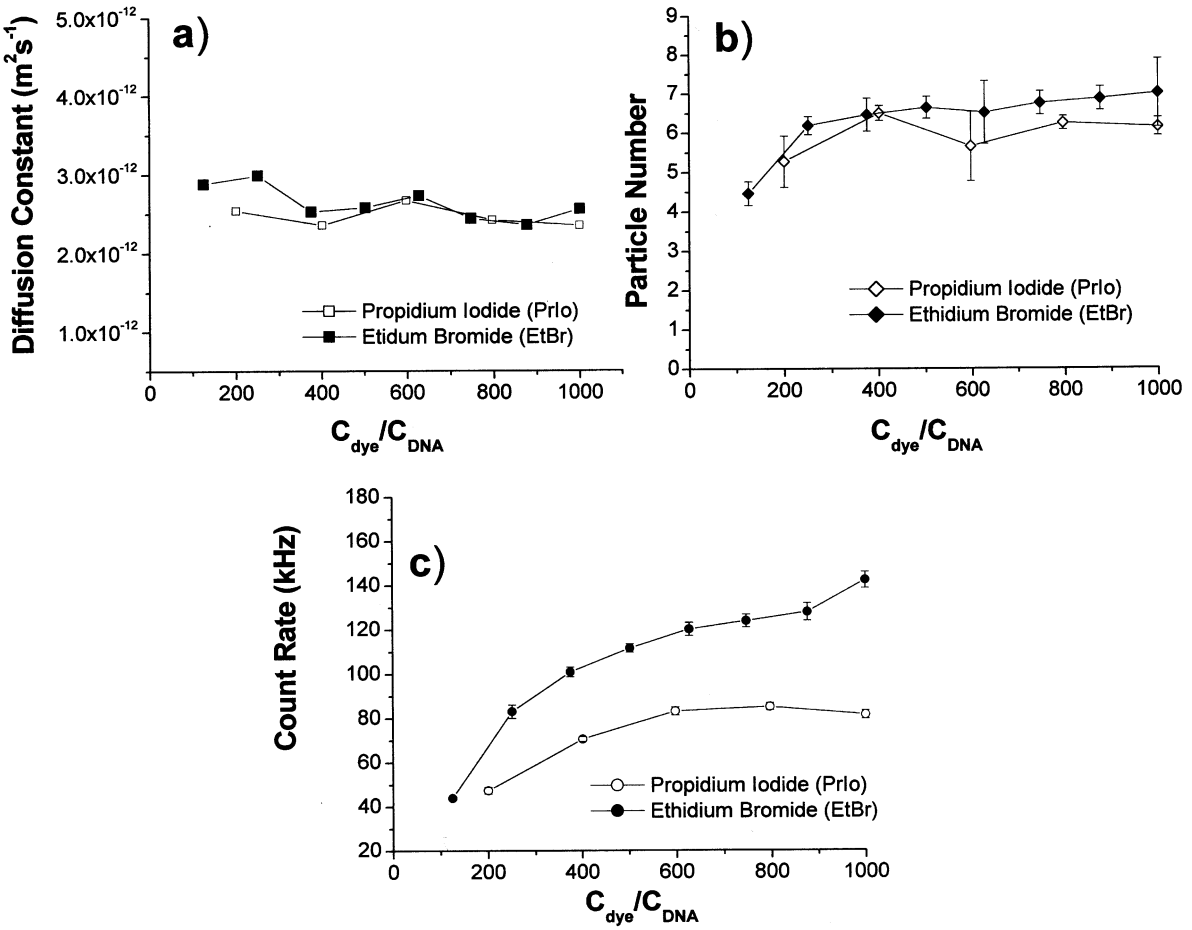

Fig. 3. Changes in the (a) diffusion constant (D), (b) particle number (N) and (c) count rate (CR) of the plasmid pBluesript SKt (2.96 kbp, contour length 1.02 μm) in the presence of increasing concentration of ethidium bromide or propidium iodide.

Both investigated DNA plasmids are semiflexibile, closed circular shape molecules. The deviation from the rigid rod-like shape certainly affects the diffusion coefficient. For a more precise theoretical estimation of the diffusion constant, in the case of our experiments measured at very low ionic strength, the worm-like chain (WLC) model would probably be the more appropriate one [26]. The aim of the paper, however, is rather the demonstration of the validity of FCS in the investigation of DNA condensation than the theoretical modelling of experimental determined diffusion constants. Anyhow, we believe that the here presented estimation of diffusion constants can be helpful when an assignment of diffusion coefficients determined by FCS to DNA molecules of particular contour length is needed.

3.2. Measurements of the DNA plasmids condensation

The condensations of both plasmids, pHβAPr-1-neo (10 kbp, contour length 3.4 μm) and p-Bluesript SKt (2.96 kbp, contour length 1.02 μm) have been measured using ethidium bromide and propidium iodide fluorescent probes. The chosen ratio C_{dye}/C_{DNA} was equal to 400 for propidium iodide and ethidium bromide. Such concentrations ensure a saturated level of DNA labeling.

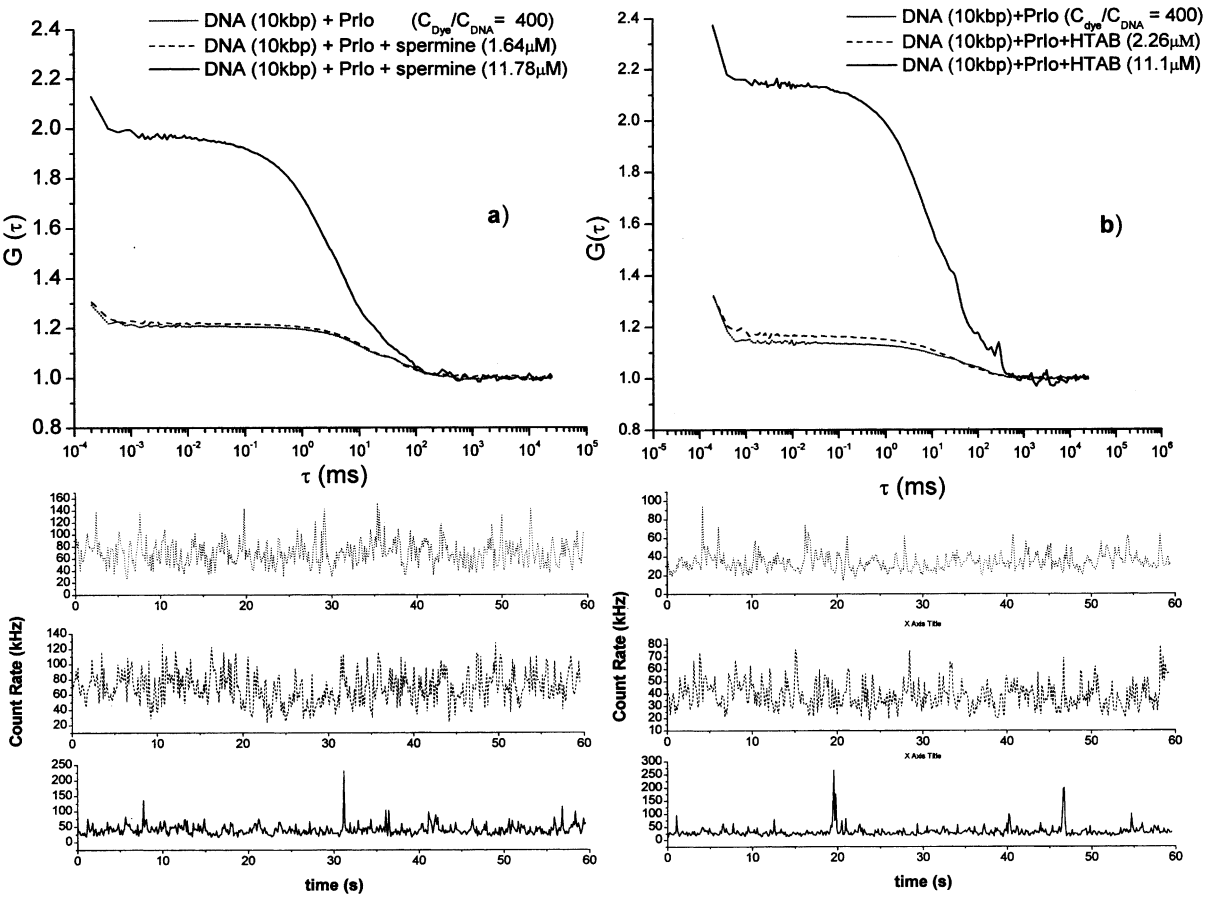

Fig. 4. Normalized fluorescence autocorrelation functions obtained for plasmid pHβAPr-1-neo (10 kbp, contour length 3.4 μm) labeled with propidium iodide measured alone (dotted line) and at two spermine (1.64 and 11.78 μM; panel a) and two HTAB (2.26 and 11.1 μM; panel b), concentrations. The C_{dye}/C_{DNA} ratio was equal to 400. Corresponding fluorescence count rates are shown on the lower panels.

It has been observed that the condensing agent concentration required to condense either one of the plasmids depends on fluorescent dye concentration (data not shown). At least two explanations of this phenomenon are possible: the dye and condensing compound interact, thus reducing their ability to associate with the DNA molecule, or (more likely) the fluorescent dye and condensing agent compete for binding sites on the plasmids. In fact, it has been observed that adsorbed fluorescent dye remains attached to the DNA molecule even after the condensation process has been completed. This is also supported by our observation that count rate and the number of fluorescent particles never disappear completely.

In order to condense plasmid, two common cationic polyions were used: naturally occurring spermine; and amphiphilic detergent HTAB. Typical count rates and corresponding normalized autocorrelation functions, for the chosen concentration of the spermine and HTAB compound, are presented in Fig. 4. Fig. 5a shows the dependence of the diffusion constant vs. spermine and HTAB concentration. When spermine or HTAB concentration was lower than 6.0×10^{-6} M, the diffusion constant of the larger plasmid (pHβAPr-1-neo, 10

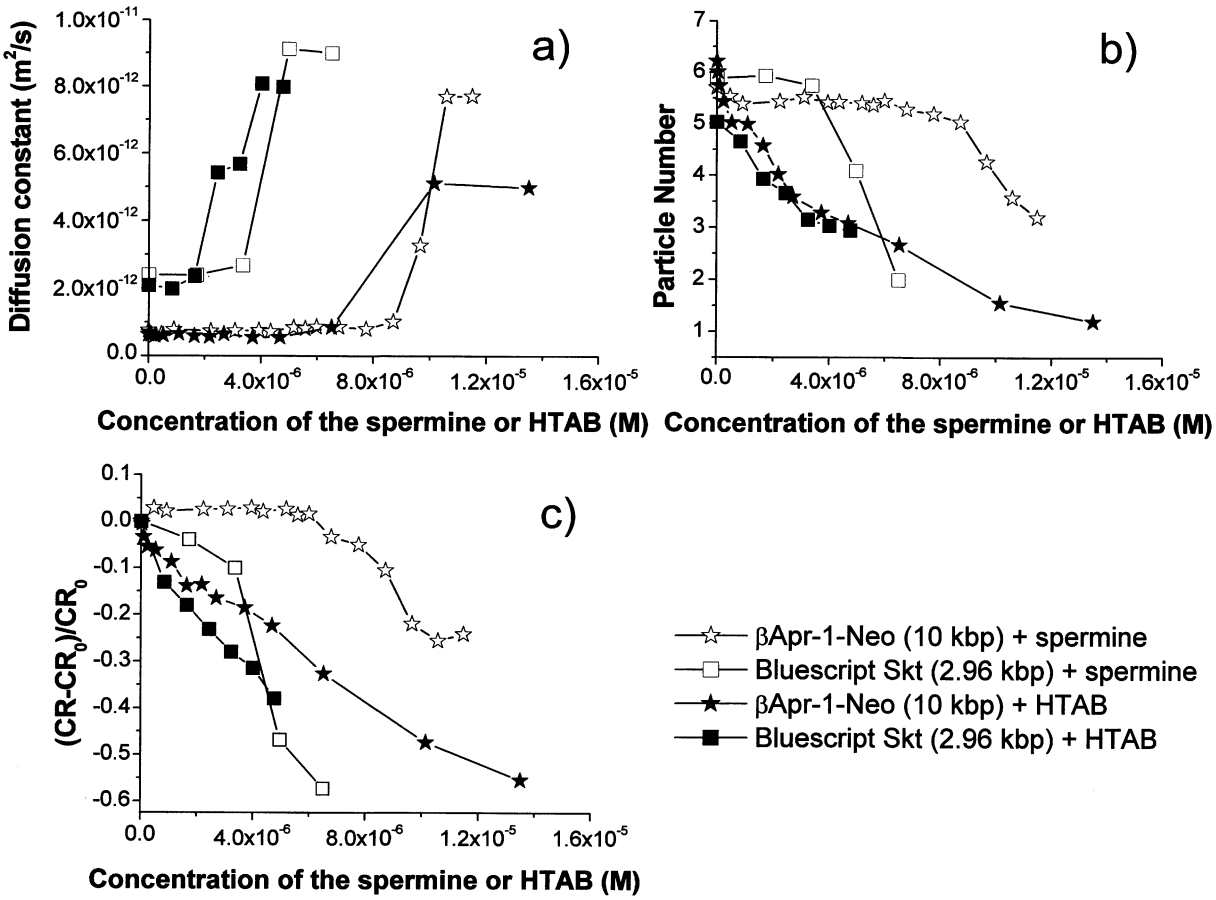

Fig. 5. Changes in the (a) diffusion constant (D), (b) particle number (N) and (c) relative count rate $[(CR-CR_0)/CR_0]$ of the plasmid pBluesript SKt (2.96 kbp; contour length, 1.02 μm; molecular mass, 1.98×10^6) and pHβAPr-1-neo (10 kbp; contour length, 3.4 μm; molecular mass, 6.6×10^6) as a dependence of a concentration of the spermine and HTAB compounds. Both plasmids were labeled by the propidium iodide. The C_{dye}/C_{DNA} ratio was equal to 400.

kbp) remained constant at $D_{10\ kbp}=9.6\times10^{-13}$ $m^2\ s^{-1}$. The smaller plasmid pBluesript SKt (2.96 kbp) diffusion constant also remained constant for condensing agents concentrations lower than 2.0×10^{-6} M, and was $D_{2.96\ kbp}=2.5\times10^{-12}$ $m^2\ s^{-1}$. Further increase in HTAB or spermine concentration causes increase of the diffusion constant, indicating the collapse of an individual plasmid to small compact particles, i.e. globular state.

When the concentration of condensing agents is higher than 1.1×10^{-5} M the 10 kbp plasmid is in the condensed globular state with the diffusion constants $D_{10\ kbp}=5.5\times10^{-12}$ $m^2\ s^{-1}$ (HTAB) and $D_{10\ kbp}=8.0\times10^{-12}$ $m^2\ s^{-1}$ (spermine). Concentrations of spermine and HTAB higher than 4×10^{-6} M were sufficient to get condensed globular state in the case of the shorter plasmid (2.96 kbp). The obtained diffusion constants were equal to $D_{2.96\ kbp}=8.2\times10^{-12}$ $m^2\ s^{-1}$ (HTAB) and $D_{2.96\ kbp}=9.2\times10^{-12}$ $m^2\ s^{-1}$ (spermine). At the above mentioned concentration ranges of condensing agents the autocorrelation function could be satisfactorily fitted by a model assuming a single population of DNA molecules [Eq. (1)]. When a model assuming two distinct populations was applied, the resulting diffusion times τ_{d1} and τ_{d2} have been identical.

For the condensing agent concentration range in which the collapse takes place (e.g. between 2 and 5×10^{-6} M of the spermine for the 2.96 kbp

plasmid), the obtained autocorrelation functions could again satisfactorily fitted by a one component model. Application of the two component model did not lead to a significant improvement of the fit, but in contradiction to the above discussed concentration regions of condensing agents, yielded two diffusion times τ_{d1} and τ_{d2} with different values. This result might be interpreted in terms of the presence of two diffusing species. Obtained values of the two diffusion constants could then reflect the coexistence of the extended and globular plasmid forms [27]. On the other hand, the fact that the quality of the fits did not improve by adding a second component to Eq. (1) might indicate a rather broad size distribution of both DNA forms. Considering the described ambiguity concerning the correct model in this concentration range, we decided to show the results obtained from the monocomponent fits in Fig. 4 and Fig. 5.

It should be underlined, that the differences between diffusion times and, thus, between diffusion constants before and after condensation caused by spermine or HTAB are dramatic. This fact might be illustrated by the observation that condensation leads to a decrease in diffusion time of up to an order of magnitude. To the best of our knowledge this is the largest change in τ_d for conformational alternation in macromolecules observed so far.

In addition, there is also a noticeable difference between the final diffusion constants of plasmid globular states induced by spermine and HTAB. The diffusion constants of the spermine condensed DNA molecule were $D_{10\ kbp}=8.0\times10^{-12}\ m^2\ s^{-1}$ and $D_{2.96\ kbp}=9.2\times10^{-12}\ m^2\ s^{-1}$, whereas when HTAB was used as a condensing agent, these respective values were $D_{10\ kbp}=5.5\times10^{-12}\ m^2\ s^{-1}$ and $D_{2.96\ kbp}=8.2\times10^{-12}\ m^2\ s^{-1}$.

Count rate and particle number decrease with rising condensing agent concentration, indicating progressive fluorescent probe release (Fig. 5b,c). There is a noticeable difference between changes in count rate and particle number caused by spermine and HTAB. The explanation of changes in count rate and particle number is not as straightforward as in the case of the diffusion constant and is probably due to the complex behavior of the tertiary DNA–dye–agent aggregate. Differences between the condensation processes caused by spermine and HTAB are not easily explainable with the experimental data available at present. It can only be hypothesized that hydrophilic spermine acts more like a polycation, whereas amphiphilic HTAB interacts with plasmid in a more complex manner [9,27].

Presented data show that FCS is a technique that provides valuable information regarding processes that occur during macromolecular interactions. It correctly describes changing DNA molecule size during the condensation process. Available data show that FCS provides information concerning single molecule behavior in a statistical manner. Unlike steady-state fluorescence spectroscopy and microscopic techniques, this method is not prone to errors associated with the sampling procedure. Yet a number of problems referring to theoretical models, data processing and the interpretation of certain parameters such as count rate and particle number require further investigations.

Acknowledgments

T.K., M.B., M.L. and M.H. are acknowledging the financial support obtained by the Czech Ministry of Education (via LN 00A032), State Committee for Scientific Research, Warszawa, Poland (PBZ-04/PO4/98) and Agriculture University (336/GW/00).

References

[1] A. Coonrod, F.Q. Li, M. Horwitz, On the mechanism of DNA transfection: efficient gene transfer without viruses, Gene Ther. 4 (1997) 1313–1318.
[2] P.L. Felgner, Nonviral strategies for gene therapy, Sci. Am. 276 (1997) 102–109.
[3] G. Romano, C. Pacilio, A. Giordano, Gene transfer technology in therapy: current applications and future goals, Stem Cells 17 (1999) 191–195.
[4] T.J. Anchordoquy, G.S. Koe, Physical stability of nonviral plasmid-based therapeutics, J. Pharm. Sci. 89 (2000) 289–296.
[5] S.J. Eastman, C. Siegel, J. Tousignant, A.E. Smith, S.H. Cheng, R.K. Scheule, Biophysical characterization of cationic lipid:DNA complexes, Biochim. Biophys. Acta 1325 (1997) 41–49.
[6] V. Oberle, U. Bakowsky, I.S. Zuhorn, D. Hoekstra, Lipoplex formation under equilibrium conditions reveals a three-step mechanism, Biophys. J. 79 (2000)

1447–1453.
[7] A.D. Miller, Cationic liposomes for gene therapy, Angew Chem. Int. Ed. 37 (1998) 1768–1776.
[8] V.A. Bloomfield, DNA condensation, Curr. Opinion Struct. Biol. 6 (1996) 334–342.
[9] V.A. Bloomfield, DNA condensation by multivalent cations, Biopolymers 44 (1997) 269–278.
[10] S.M. Mel'nikov, R. Dias, Y.S. Mel'nikova, E.F. Marques, M.G. Miguel, B. Lindman, DNA conformational dynamics in the presence of cationic mixtures, FEBS Lett. 453 (1999) 113–119.
[11] D. Matulis, I. Rouzina, V.A. Bloomfield, Thermodynamics of DNA binding and condensation. Isothermal titration calorimetry and electrostatic mechanism, J. Mol. Biol. 296 (2000) 1053–1059.
[12] Y.S. Mel'nikova, S.M. Melnikov, J.-E. Lofroth, Physicochemical aspects of the interaction between DNA and oppositely charged mixed liposomes, Biophys. Chem. 81 (1999) 125–141.
[13] R.P. Haugland, Handbook of Fluorescent Probes and Research Chemicals. Molecular Probes, Eugene, OR, USA, 1996.
[14] S.M. Mel'nikov, V.G. Sergeyev, K. Yoshikawa, Discrete coil-globule transition of large DNA induced by cationic surfactant, J. Am. Chem. Soc. 117 (1995) 2401–2408.
[15] S.M. Mel'nikov, V.G. Sergeyev, Y.S. Mel'nikova, K. Yoshikawa, Folding of long DNA chains in the presence of distearyldimethylammonium bromide and unfolding induced by neutral liposomes, J. Chem. Soc. Faraday Trans. 93 (1997) 283–288.
[16] J. Sambrook, E.F. Fritsch, T. Maniatis, Molecular Cloning, A Laboratory Manual, Second edition, Cold Spring Harbor Laboratory Press, New York, USA, 1989, p. 121.
[17] N.L. Thompson, Topics in fluorescence spectroscopy I, in: J.R. Lakowicz (Ed.), Fluorescence Correlation Spectroscopy, 1, Plenum Press, New York, 1991, p. 337.
[18] P. Schwille, J. Bieschke, F. Oehlenschlaeger, Kinetic investigations by fluorescence correlation spectroscopy: the analytical and diagnostic potential of diffusion studies, Biophys. Chem. 6 (1997) 211–228.
[19] M. Beneš, J. Hudeček, P. Anzenbacher, M. Hof, Coumarin 6, Hypericin, Resorufins and Flavins: suitable chromophores for fluorescence correlation spectroscopy of biological molecules, Coll. Czech. Chem. Commun. 66 (2001) 855–869.
[20] R. Borsali, H. Nguyen, R. Pecora, Small-angle neutron scattering and dynamic light scattering from a polyelectrolyte solution: DNA, Macromolecules 31 (1998) 1548–1555.
[21] D.G. Wilkinson, in: D.G. Wilkinson (Ed.), In Situ Hybridization: A Practical Approach, IRL Press, 1992, p. 1.
[22] S.B. Smith, L. Finzi, C. Bustamante, Direct mechanical measurements of the elasticity of single DNA molecules by using magnetic beads, Science 258 (1992) 1122–1126.
[23] D. Magde, E. Elson, W.W. Webb, Thermodynamic fluctuations in a reacting system-measurement by fluorescence correlation spectroscopy, Phys. Rev. Lett. 29 (1972) 705–708.
[24] M. Weismann, H. Schindler, G. Feher, Proc. Natl. Acad. Sci. USA 73 (8) (1976) 2776–2780.
[25] M.M. Tirado, J. Garcia de la Torre, Rotational dynamics of rigid, symmetric top macromolecules. Application to circular cylinders, J. Chem. Phys. 73 (4) (1980) 1986–1993.
[26] C.G. Baumann, S.B. Smith, V.A. Bloomfield, C. Bustamante, Ionic effects on the elasticity of single DNA molecules, Proc. Natl. Acad. Sci. USA 94 (1997) 6185–6190.
[27] S.M. Mel'nikov, V.G. Sergeyev, K. Yoshikawa, Transition of double-stranded DNA chains between random coil and compact globule states induced by cooperative binding of cationic surfactants, J. Am. Chem. Soc. 117 (1995) 9951–9956.